DOI 10.1007/s11106-020-00158-1
Powder Metallurgy and Metal Ceramics, Vol. 59, Nos. 5-6, September, 2020 (Russian Original Vol. 59, Nos. 5-6, May-June, 2020)

NANOSTRUCTURED MATERIALS

NOVEL STRATEGY FOR ONE-STEP PRODUCTION OF ATTENUATED Ag-CONTAINING AgCu/ZnO ANTIBACTERIAL-ANTIFUNGAL NANOCOMPOSITE PARTICLES

Tolga Çakmak,[1] Elif Emil Kaya,[2] Demet Küçük,[3] Burçak Ebin,[1,4] Onur Balci,[3] and Sebahattin Gürmen[1,5]

UDC 669.225;621.6.04;52-37

Novel strategies have been developed to comply with Registration, Evaluation, Authorization, and Restriction of Chemicals (REACH) regulations to provide the same performances for antibacterial and antifungal materials. The strategy for producing composite materials by attenuating the silver (Ag) content and a one-step production technique without minimizing the antibacterial and antifungal performance was developed. In this study, attenuated spherical Ag containing spherical AgCu/ZnO nanocomposite particles have been synthesized from an aqueous solution of silver nitrate ($AgNO_3$), copper nitrate ($Cu(NO_3)_2 \cdot 3H_2O$), and zinc nitrate ($Zn(NO_3)_2 \cdot 7H_2O$) by a facile one-step ultrasonic spray pyrolysis and hydrogen reduction (USP-HR) method. Characterization of AgCu/ZnO nanocomposite particles was carried out by various techniques such as X-ray diffraction analysis (XRD), scanning electron microscopy (FEG-SEM), energy dispersive spectroscopy (EDS), and transmission electron microscopy (TEM). The structural analysis showed that AgCu/ZnO nanocomposites were composed of face-centered cubic Ag, face-centered cubic Cu, and hexagonal ZnO phases. Antibacterial and antifungal properties of nanocomposite particles against Escherichia coli and Aspergillus niger were investigated by agar medium and broth medium methods. The obtained results indicate that produced nanocomposite particles possess antibacterial and antifungal properties (100%). The attenuated Ag in the AgCu/ZnO nanocomposite particles has the usage potential in different areas of the textile industry. In particular, the research on utilizing this nanocomposite in hand-made fiber production as an additive is of very high interest.

Keywords: *nanocomposite materials, AgCu/ZnO, antibacterial and antifungal properties, spray pyrolysis.*

[1]Department of Metallurgical and Materials Engineering, Istanbul Technical University, 34469 Sariyer-Istanbul, Turkey. [2]Department of Materials Science & Tech., Turkish-German University, Beykoz-Istanbul, Turkey. [3]Department of Textile Eng., Kahramanmaras Sutcu Imam University, Kahramanmaras, Turkey. [4]Nuclear Chemistry and Industrial Material Recycling, Department of Chemistry and Chemical Eng., Chalmers University of Technology, S-412 96, Gothenburg, Sweden.

[5]To whom correspondence should be addressed; e-mail: gurmen@itu.edu.tr.

Published in Poroshkova Metallurgiya, Vol. 59, Nos. 5–6 (533), pp. 30–41, 2020. Original article submitted January 21, 2020.

INTRODUCTION

The nanocomposite is generally defined as the combination of the nanostructured materials, mostly nanoparticles, embedded in a matrix to modify and manipulate the features for enhanced effect and multifunctionality [1, 3]. In the last decades, inorganic nanocomposite particles have attracted increasing attention due to the unlimited ability to design superior materials with controllable physical and chemical properties for specific applications. They are promising candidates for application as catalyzers and photo-catalyzers in the chemical industry, as well as semiconductors and magnetic materials in electronic and aviation industries [4–7]. However, these advanced materials should be compatible with the regulations of Registration, Evaluation, Authorization, and Restriction of Chemicals (REACH) to be used in the European Union (EU). REACH is a regulation of the EU that addresses the production and use of chemical substances to reduce the possible risks and improve the protection of human health and environment [8]. Nanocomposite technology reveals new opportunities to solve bacterial and fungal health and environmental issues through advanced materials with improved antimicrobial properties for biomedical applications [6, 7, 9–14]. The desired properties of nanocomposite particles are developed by manipulating shape, particle size, chemical composition, surface composition, and surface atomic arrangement, which can be controlled by production method [15, 16].

Many methods have been used for the production of nanocomposites. Among them, the ultrasonic spray pyrolysis (USP) technique has been rarely applied for this purpose, although it is a promising method to produce metal/metal oxide nanocomposite particles since the desired chemical composition of the particles and the particle size can be controlled through process parameters. The significant factors of the USP method are precursor type, precursor concentration, reaction atmosphere, carrier gas flow rate, and reaction temperature. In addition, smaller particle size, spherical morphology, and chemical uniformity of particles are the other advantages of the method [16–21]. Spherical silver/zinc oxide (Ag/ZnO) nanocomposite particles were produced at 700–900°C by the USP process using an aqueous solution of silver nitrate and zinc nitrate as a precursor under 0.5 L/min air flow for photocatalytic applications [16]. This method was also applied to prepare Fe/metal oxide nanocomposite particles at 600 and 800°C from an aqueous solution containing magnesium nitrate and iron (III) nitrate using hydrogen as a carrier gas and reducing agent [20].

Numerous studies on the application of antifungal and antibacterial materials have been performed in recent years [22]. Silver (Ag), copper (Cu), and zinc oxide (ZnO) have become the focus of such intensive research due to their antifungal and antibacterial properties against preventing the growth of bacteria and fungus [13, 23]. Copper is known to be used to prevent the formation of algae at the bottom of vessels since very early times [22–24]. Nowadays, it is used to inhibit microbial growth in the medical and the textile industry [25, 26]. Similarly, Ag is used as an antibacterial agent in textile industry, medical devices, and surface coating of metals and polymers [27–31]. Recently, the ZnO-based nanostructures have attracted considerable interest due to antimicrobial activities against bacteria [32]. Ultimately, concerning lower costs, atmospheric stability of the material, compatibility with human skin, and self-cleaning ability of ZnO nanoparticles, the comparison with Ag nanoparticles is quite reasonable [33, 34]. Moreover, the shape and the size of the nanocomposite particles considerably influence the antibacterial and antifungal properties, and the nanoparticles have been proven to express the strongest bactericide influence [32].

The purpose of this study was to develop an antifungal and antibacterial nanocomposite material with reduced Ag content, which can be used in advanced textile products. Since no previous studies have been reported on the synthesis of AgCu/ZnO nanocomposite by ultrasonic spray pyrolysis and hydrogen reduction (USP-HR) method, this study aimed at preparing the antifungal and antibacterial particles in a single-step way with a controlled Ag content and particle morphology. The properties of the samples were analyzed to investigate the effects of the Ag content in the particles on their antibacterial and antifungal performance.

EXPERIMENTAL PROCEDURE

AgCu/ZnO nanocomposite particles were synthesized utilizing an aqueous solution of silver nitrate ($AgNO_3$), copper nitrate ($Cu(NO_3)_2 \cdot 3H_2O$), and zinc nitrate ($Zn(NO_3)_2 \cdot 7H_2O$) under 500 mL/min H_2 flow rate at 600°C reduction temperature. The nitrate salts (all from Merck) were dissolved in deionized water and stirred by a

TABLE 1. Experimental Parameter

Code	Ag^{+} (M)	Cu^{2+} (M)	Zn^{2+} (M)	Temperature, °C
S1	0.1	0.1	0.1	600
S2	0.025	0.1	0.1	600
S3	0.025	0.2	0.2	600
S4	0.025	0.2	0.4	600

magnetic mixer for 30 min. Metal concentration in the precursor was between 0.025 and 0.4 mol/L. Details of the experimental parameters for the synthesis of AgCu/ZnO nanocomposite particles are given in Table 1. Nitrogen with a 250 mL/min flow rate was used to remove the oxygen and create an inert atmosphere in the experimental set-up before and after the reduction process due to the safety regulations. The precursor was atomized by an atomizer frequency with 1.3 MHz into a fine mist and carried into the preheated furnace by 500 mL/min hydrogen gas flow. The reduction of aerosol droplets occurred at 600°C in the electrically heated furnace with the heating zone of 0.25 m and the diameter of the quartz tube of 0.02 m.

X-ray diffraction patterns were obtained for crystal structure determination of alloy particles by Philips-1700 X-ray diffractometer applying the Cu-K_{α} radiation. The AgCu/ZnO nanocomposite particle morphology was revealed by field emission scanning electron microscopy (FE-SEM, Jeol JSM 700F). The synthesized nanocomposite powders were first dispersed in ethanol and inserted in an ultrasonic bath for 15 min. Afterward, the suspension was placed dropwise into a brass sheet to obtain a thick film, which later was coated by platinum for scanning electron microscopy (SEM) analysis. Chemical compositions of particles were analyzed by energy dispersive spectroscopy (EDS). Besides, particle size and morphology of the samples were investigated by transmission electron microscopy (Jeol JEM-2200FS TEM). The AgCu/ZnO nanocomposite particles in ethanol for TEM analyses were drop-cast onto the molybdenum TEM grid and then used for analyses.

The antibacterial and antifungal activities of AgCu/ZnO nanocomposite particles were evaluated according to ASTM E 2149-01 and AATCC 30 standard test methods. ASTM E 2149-01 test method is applied to determine the antimicrobial activity of immobilized antimicrobial agents under dynamic contact conditions. The AgCu/ZnO nanocomposite particles were evaluated for the antibacterial performance against *E. coli*. The bacterial concentration transferred to each sample weighing 1 g was calculated as 4.15 × 105 colony-forming unit (CFU). The bacterial cultures were incubated for 24 h at 37°C. The reduction in bacterial counts was determined by visual observation. AATCC test method is preferred to evaluate the resistance of materials against mold and rot. In this method, samples are incubated with *Aspergillus niger* fungus in a petri dish, and eventually, the presence and absence of bacteria are investigated in the samples. A 1 mL solution containing antibacterial material was dropped on the prepared fungus to indicate the inhibition activity of nanocomposite particles, and a clear area around the nanocomposites was detected after one day. The reduction in *Aspergillus niger* counts was determined by comparing the control specimen.

RESULTS AND DISCUSSION

Thermodynamic Analysis of Ag, Cu, and ZnO Nitrate Salts. The thermodynamic reaction for hydrogen reduction of Ag, Cu, and ZnO nitrate salts can be described as in Eqs. (1)–(3):

$$AgNO_3 + H_{2(g)} \rightarrow Ag + H_2O + NO_{2(g)}, \quad (1)$$

$$Cu(NO_3)_2 + 2H_{2(g)} \rightarrow Cu + 2H_2O + 2NO_{2(g)}, \quad (2)$$

$$Zn(NO_3)_2 + 2H_{2(g)} \rightarrow ZnO + 2H_2O + 2NO_{2(g)}. \quad (3)$$

The thermodynamic expectation was computed by HSC software. Figure 1 shows the Gibbs free energy for the temperature range of 0–1000°C. As can be seen, the Gibbs free energy is negative between 0 and 1000°C. This allows for silver and copper to be formed by the hydrogen reduction of silver and copper nitrates and zinc oxide by decomposition of zinc nitrate, which is energetically favored at 600°C.

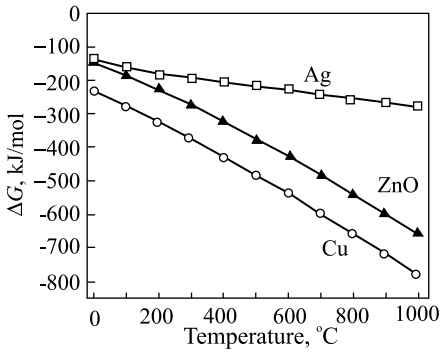

Fig. 1. Gibbs free energy change of decomposition reaction for silver, copper, and zinc nitrate at elevated temperatures

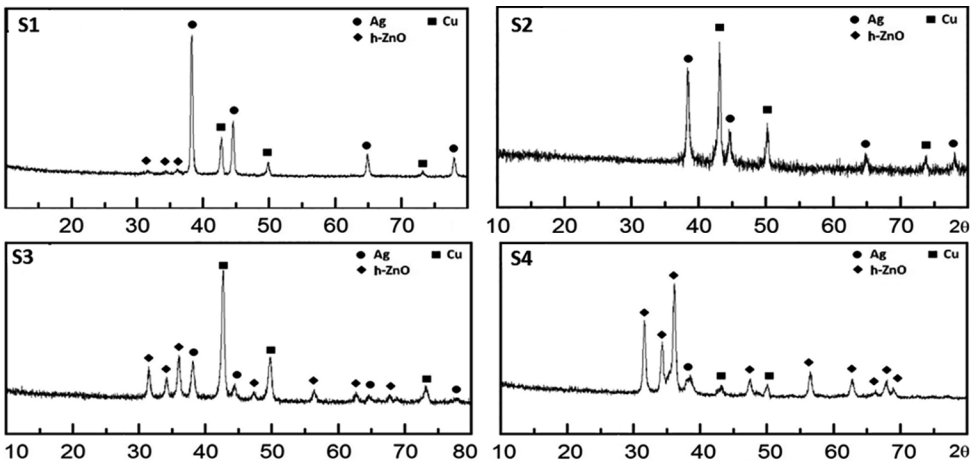

Fig. 2. XRD analyses of AgCu/ZnO nanocomposite particles: the codes S1, S2, S3, and S4 are described in Table 1

Structural Characterization of AgCu/ZnO Nanocomposite Particles. The X-ray diffraction patterns of AgCu/ZnO nanocomposite particles were recorded in the range of 20–80° and given in Fig. 2. The peak at 2θ = = 38.08°, 44.36°, 64.26°, and 77.30° are assigned to the (111), (200), (220), and (311) reflection lines, respectively, which confirms the formation of the face-centered cubic structure of Ag corresponding to JCPDS Card No. 01-087-0719. The FCC Cu-phase at 2θ = 43.64°, 50.80°, and 74.42° coincide with (111), (200), and (220), respectively, which is following the JCPDS Card No. 04-0836. The planes (100), (002), (101), (102), (110), (103), (112), (201), and (202) of hexagonal wurtzite ZnO phase are observed at 2θ = 31.74°, 34.37°, 36.23°, 47.37°, 56.68°, 62.88°, 67.97°, and 69.13°, respectively, which comply with the JCPDS Card No. 01-079-2205. Although ZnO peaks are slightly observed for sample Ag : Cu : Zn = 0.1 : 0.1 : 0.1, its' diffraction pattern disappeared with the decrease in Ag concentration to 0.025 M. Thus, a low amount of Ag did not show any catalytic effect on the decomposition reaction of the $Zn(NO_3)_2$ to ZnO. When Zn^{2+} concentration was increased in the precursor from 0.1 M to 0.4 M, the XRD peaks of ZnO became more apparent. Results show that AgCu/ZnO nanocomposite particles were synthesized successfully, and no other phases, such as decomposed nitrate phases, were detected in the samples. Although the EDS analysis of the sample S2 (Ag^{+}:0.025 M, Cu^{2+}:0.1 M, and Zn^{2+}:0.1 M) in Figs. 3 and 4 showed the existence of Zn in the sample, and no ZnO peaks were observed in the XRD patterns.

Morphological Characterization of AgCu/ZnO Nanocomposite Particles. The morphology of AgCu/ZnO nanocomposite was revealed by SEM (Fig. 5) and TEM analysis (Fig. 4). Figure 5 shows the SEM micrographs of AgCu/ZnO nanocomposite particles prepared by the USP method from Cu, Ag, and Zn nitrate salts at 600°C. It is seen that the molar ratio of Cu, Ag, and Zn nitrate salts in the precursor affect the morphology of nanocomposite particles.

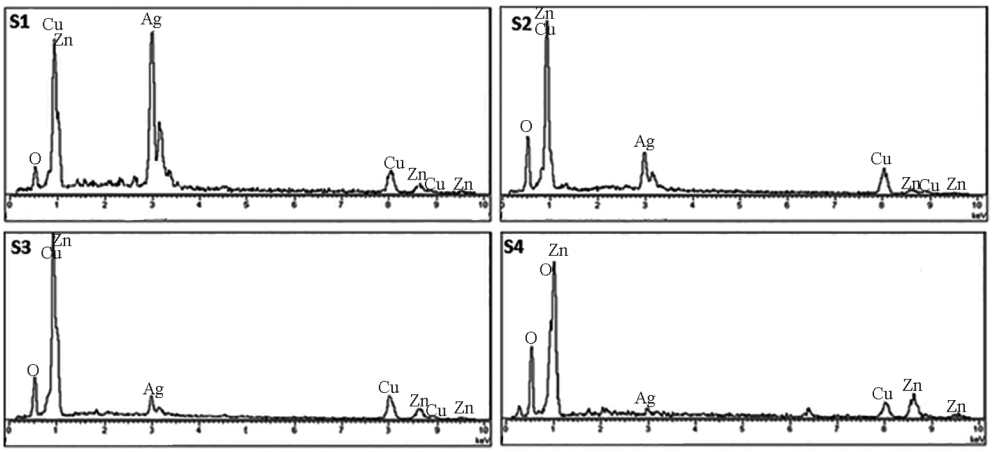

Fig. 3. EDS analyses of AgCu/ZnO nanocomposite particles

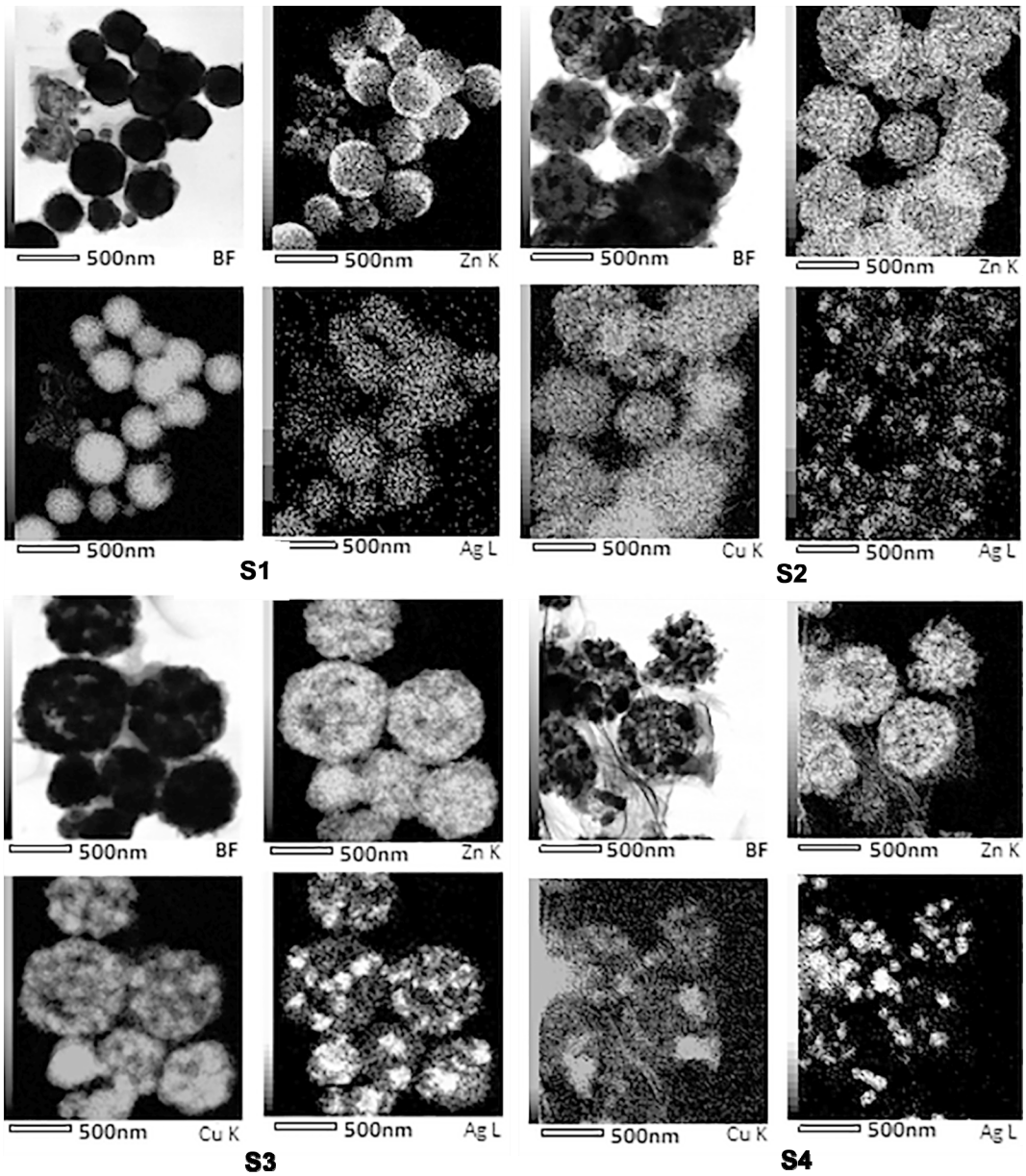

Fig. 4. TEM and EDS mapping results of AgCu/ZnO nanocomposite particles

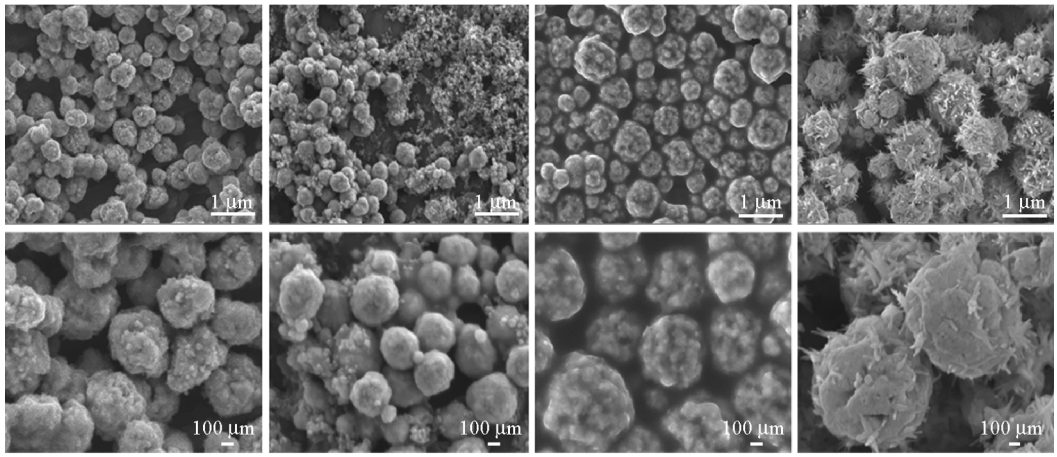

Fig. 5. SEM analyses of AgCu/ZnO nanocomposite particles

As seen from SEM images, metallic silver could have a binder effect for the nanocomposite particles at 600°C because the reaction temperature was higher than the Tammann temperature (half of the melting temperature) of Ag (T_m, Ag ~ 962), which is considered as the beginning of effective sintering. All samples exhibit nearly spherical morphology. However, as the concentration of Zn increases, the surface morphology of nanocomposite particles seems to be needled due to the hexagonal growth of ZnO nanostructures. EDS analyses of the nanocomposite particles are given in Fig. 3.

The presence of Ag, Cu, Zn, and O was affirmed by EDS analysis. Any possible impurities, such as nitrogen, were not detected in the EDS spectrums due to undecomposed reactants. Table 2 shares the atomic percentages of the confirmed elements and chemical composition of the samples nearly the same with the starting solution concentrations.

TEM analyses clearly indicate that size of AgCu/ZnO nanocomposite particles is in the submicron size range between 350 and 800 nm. These particles were formed by aggregation of the primary nucleated nanostructured crystallite with the range around 20 to 40 nm. The spherical nanocomposite particles consisting of Ag, Cu, and ZnO show a quite uniform distribution in accordance with elemental mapping analyses as shown in Fig. 4.

TABLE 2. Chemical Composition (at.%) of AgCu/ZnO Nanocomposite Particles

Code	Ag	Cu	Zn	O
S1	23.83	21.24	10.89	44.03
S2	8.78	35.34	8.07	47.81
S3	3.87	28.09	19.01	49.04
S4	1.16	15.80	33.34	49.71

TABLE 3. The Value of Antibacterial Activity of Nanocomposite Against *E. coli* Bacteria after 24 h

The code of specimen	Bacterial reduction, %	The code of specimen	Bacterial reduction, %
Untreated reference sample	+ 140.96	2	– 100.00
1	– 100.00	3	– 100.00
		4	– 100.00

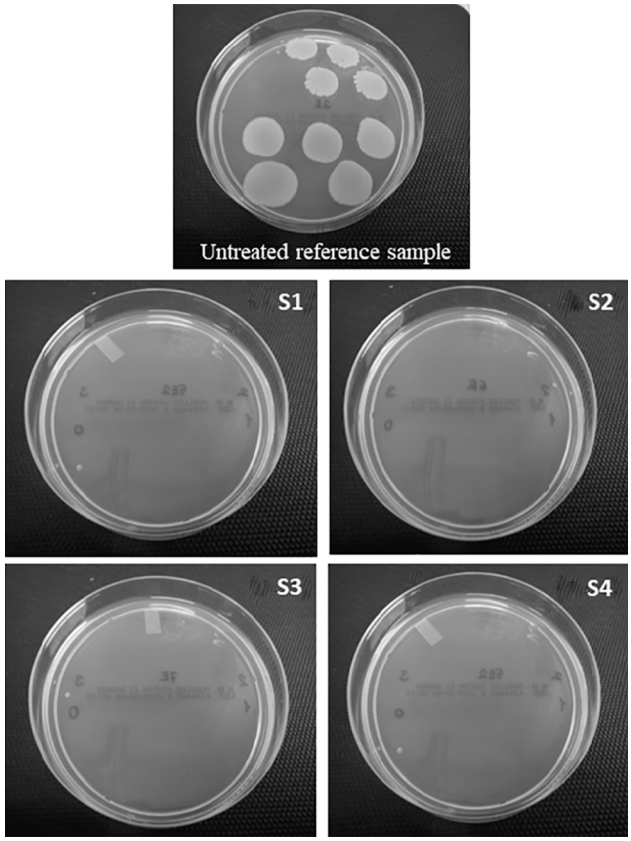

Fig. 6. Antibacterial activity measurement of AgCu/ZnO nanoparticles

Antibacterial and Antifungal Properties of AgCu/ZnO Nanocomposite Particles. The measurements of antibacterial and antifungal performance were made with AgCu/ZnO specimens showed in Table 1. The antibacterial activity of the nanocomposite materials defined in Table 1 was assessed against *E. coli* (gram-negative) bacteria (ATCC 35218) via planting the bacteria to the agar medium under dynamic contact conditions according to ASTM E 2149-01 standard. The measurement was performed after incubation at 37ºC for 24 hours. This test standard is suitable for this kind of particles which do not tend to migrations. The antibacterial activity of these particles against *E. coli* bacteria is presented in Table 3 and Fig. 6.

In order to accept a sample as antibacterial, bacterial growth should not occur around, above, or below the sample. Besides, the size of the protection zone of the sample was the signal for the antibacterial activity. When examining Fig. 6, it was established that bacteria did not grow. The results given in Table 3 and Fig. 6 allow stating that the produced nanoparticles have high and significant antibacterial performance.

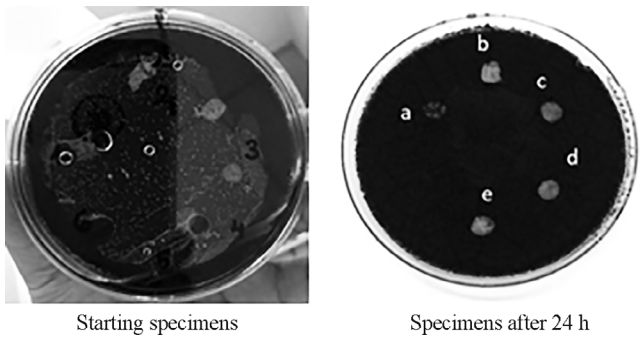

Fig. 7. Antifungal performance of specimens according to AATCC 30 method against *Aspergillus niger*: a) control specimen; b, c, d, and e) code 1, 2, 3, and 4, respectively

The antifungal activities of the particles were tested against *Aspergillus niger* fungi via planting the bacteria to the agar medium according to AATCC 30 Standard. Similar to antibacterial activity assessment, in order to accept a sample as antifungal, bacterial growth should not occur around, above, or below the sample, and the increment in the size of the protection zone of the sample was the signal that the antifungal activity increased. The test results of novel nanocomposites are given in Fig. 7.

The results of comparing the control sample and produced particles allow stating that the samples showed high antifungal activity due to no fungal growth under and around the particles. Also, the level of the activity demonstrated differences depending on the chemical structure of particles.

CONCLUSIONS

AgCu/ZnO nanocomposite particles were successfully synthesized via hydrogen reduction assisted by ultrasonic spray pyrolysis method in one step at 600°C using an aqueous solution of silver/copper/zinc nitrates as a precursor. The amount of silver was reduced in the developed nanocomposite material following its cost and ecotoxicological effects. The effects of various precursor concentration on the morphology and crystal structure of the AgCu/ZnO nanocomposite particles were investigated.

Electron microscopy studies revealed that the primary nucleated particle sizes of nanocomposites vary between 20 and 40 nm, and aggregation of the primary particles formed the nanocomposite particles with a size range between 350 to 800 nm with uniform morphologies. The elemental composition of the particles can be controlled by changing the metal concentrations of the precursor solutions, and resulted composition has homogeneous distribution in the particle structure.

The prepared nanocomposite particles consist of three crystal structures, which are face-centered cubic Ag, face-centered cubic Cu, and hexagonal ZnO phases. Furthermore, the elimination of 100% bacteria was achieved by all synthesized nanocomposite samples. According to the solid medium and liquid medium test methods, they have also antifungal properties.

The antibacterial and antifungal activity of nanocomposite was not negatively affected by decreased Ag concentration in precursor due to the positive impact of the Cu and ZnO. Moreover, it is worth emphasizing that textile applications of nanocomposites synthesized by reducing silver content are promising to eradicate the target bacteria and fungi.

Improved antibacterial (ASTM E 2149-01) and antifungal (AATCC 30) performance of AgCu/ZnO nanocomposite particles demonstrated that AgCu/ZnO nanocomposite particles could be used as antibacterial and antifungal agents in various area.

ACKNOWLEDGEMENTS

This research has been funded by Turkish Scientific and Technological Research Council (TUBITAK) with a grant number TUBITAK-213M267. Authors also thank Prof. Dr. Gultekin Goller, Dr.-Ing. Ikbal Isik, and Technician Huseyin Sezer for SEM, TEM, and XRD characterizations.

REFERENCES

1. Saima Sultana, Rafiuddin, Mohammad Zain Khan, Khalid Umar, and M. Muneer, "Electrical, thermal, photocatalytic and antibacterial studies of metallic oxide nanocomposite doped polyaniline," *Electrical, Thermal. J. Mater. Sci. Technol.*, **29**, 795–800 (2013); doi.org/10.1016/ j.jmst.2013.06.001.
2. J. Jose and M.A. Khadar, "Role of grain boundaries on the electrical properties of ZnO–Ag nanocomposites: an impedance spectroscopic study," *Acta Materialia.*, **49**, 729–735 (2001); doi.org/10.1016/S1359-6454(00)00369-4.
3. B. Houng and C.-J. Huang, "Structure and properties of Ag embedded aluminum doped ZnO nanocomposite thin films prepared through a sol–gel process," *Surf. Coat. Tech.*, **201**, 3188–3192 (2006); doi: 10.1016/j.surfcoat.2006.06.043.

4. F. Petronella, A. Truppi, C. Ingrosso, T. Placido, M. Striccoli, M.L. Curri, A. Agostiano, and R. Comparelli, "Nanocomposite materials for photocatalytic degradation of pollutants," *Catal. Today.*, 281, 85–100 (2017); doi.org/10.1016/j.cattod.2016.05.048.
5. Bibha Boro, B Gogoi, BM Rajbongshi, and A Ramchiary, "Nano-structured TiO_2/ZnO nanocomposite for dye-sensitized solar cells application: A review," *Renewable and Sustainable Energy Reviews*, **81**, 2264–2270 (2018).
6. Xue-Gang Chen, Ji-Peng Cheng, Shuang-Shuang Lv, Ping-Ping Zhang, Shu-TingLiu, and Ying Ye, "Preparation of porous magnetic nanocomposites using corncob powders as template and their applications for electromagnetic wave absorption," *Composite Sci. Technol.*, **8**, Issue 8, 908–914 (2012); doi.org/10.1016/j.compscitech.2012.03.001.
7. P. Mendoza Zélis, M.B. Fernández van Raap, L.M. Socolovsky, A.G. Leyva, and F.H. Sánchez, "Magnetic hydrophobic nanocomposites: Silica aerogel/maghemite," *Physica B.*, **407**, Issue 16, 3113–3116 (2012). doi.org/10.1016/j.physb.2011.12.039.
8. *European Chemical Agency*; https://echa.europa.eu/regulations/reach/understanding-reach Last Acces: 15.05.2018.
9. G. Gu, J. Xu, Y. Wu, M. Chen, and L. Wu, "Synthesis and antibacterial property of hollow SiO_2/Ag nanocomposite spheres," *Journal of Colloid and Interface Science***, 359**, 327–333 (2011); DOI: 10.1016/j.jcis.2011.04.002.
10. Elayaraja Kolanthai, P. Abinaya Sindu, K. Thanigai Arul, V. Sarath Chandra, E. Manikandan, S. Narayana Kalkura, "Agarose encapsulated mesoporous carbonated hydroxyapatite nanocomposites powder for drug delivery," *Journal of Photochemistry and Photobiology. B, Biology,* **166**, 220–231 (2016); doi: 10.1016/j.jphotobiol.2016.12.005.
11. A.O. Juma, E.A.A. Arbab, C.M. Muiva, L.M. Lepodise, and G.T. Mola, "Synthesis and characterization of CuO-NiO-ZnO mixed metal oxide nanocomposite," *J. Alloys Compd.*, **723**, No. 5, 866–872 (2017); doi.org/10.1016/j.jallcom.2017.06.288.
12. C. Marambio-Jonesand, E.M.V. Hoek, "A review of the antibacterial effects of silver nanomaterials and potential implications for human health and the environment," *J. Nanoparticle Res.*, **12**, 531–1551(2010); doi:10.1007/s11051-010-9900-y.
13. M. Elango, M. Deepa, R. Subramanian, and A.M. Musthafa, "Synthesis, characterization of polyindole/ AgZnO nanocomposites and its antibacterial activity," *J. Alloys Compd.*, **696**, 391–401 (2017); doi.org/10.1016/j.jallcom.2016.11.258.
14. S. Azizi, R. Mohamad, R.A. Rahim, A.B. Moghaddam, M. Moniri, A. Ariff, W.Z. Saad, and F. Namvab, "ZnO–Ag core shell nanocomposite formed by green method using essential oil of wild ginger and their bactericidal and cytotoxic effects," *Appl. Surf. Sci.*, **384**, 517–524 (2016); doi.org/10.1016/j.apsusc.2016.05.052.
15. R.W. Siegel, Nanophase Materials: Synthesis, Structure, and Properties, in: *Physics of New Materials* (1994), pp. 65–105.
16. K.B. Dermenci, B. Genc, B. Ebin, T. Olmez-Hanci, and S. Gürmen, "Photocatalytic studies of Ag/ZnO nanocomposite particles produced via ultrasonic spray pyrolysis method," *J. Alloys Compd.*, **586**, 267–273 (2014); doi.org/10.1016/j.jallcom.2013.10.004.
17. E. Emil and S. Gurmen, "Estimation of yttrium oxide microstructural parameters using the Williamson–Hall analysis," *Mater. Sci. Technol*., **836**, 1549–1557 (2018); DOI: 10.1080/02670836.2018.1490857.
18. B. Ebin, G. Lindbergh, and S. Gurmen, "Preparation and electrochemical properties of nanocrystalline $LiB_xMn_{2-x}O_4$ cathode particles for Li-ion batteries by ultrasonic spray pyrolysis method," *J. Alloys Compd.*, **620**, 399–406 (2015); doi.org/10.1016/j.jallcom.2014.09.098.
19. E. Emil, G. Alkan, S. Gurmen, R. Rudolf, D. Jenko, and B. Friedrich, "Tuning the Morphology of ZnO Nanostructures with the Ultrasonic Spray Pyrolysis Process," *Metals.*, **8**, 569 (2018); doi.org/10.3390/met8080569.

20. B. Ebin, C. Toparli, and S. Gurmen, “Preparation and magnetic characterization of Fe/metal oxide nanocomposite particles by means of hydrogen reduction assisted ultrasonic spray pyrolysis (USP-HR),” *Int. J. Mater. Res.* **104**, 483–488 (2013); doi.org/10.3139/146.110883.
21. E. Emil Kaya, O. Kaya, G. Alkan, S. Gurmen, S. Stopic, B. Friedrich, “New proposal for size and size-distribution evaluation of nanoparticles synthesized via ultrasonic spray pyrolysis using search algorithm based on image-processing technique,” *Materials.*, **13**, 38 (2020); doi.org/10.3390/ma13010038.
22. N. Cioffi and M. Rai, *Nano-Antimicrobials Prog*. Prospect. 9783642244 (2012), 556 p.
23. Q. Yu, X. Xu, C. Wang, Y. Ma, D. Hui, and Z. Zhou, “Remarkably improvement in antibacterial activity by synergistic effect in n-Cu@T-ZnO nanocomposites,” *Compos. Part B-Eng.*, **110**, 32–38 (2017); doi.org/10.1016/j.compositesb.2016.10.085.
24. M.S. Usman, M.E. El Zowalaty, K. Shameli, N. Zainuddin, M. Salama, and N.A. Ibrahim, “Synthesis, characterization, and antimicrobial properties of copper nanoparticles,” *Int. J. Nanomedicine.*, **8**, 4467–4479 (2013); doi: 10.2147/IJN.S50837.
25. N.S. Heliopoulos, S.K. Papageorgiou, A. Galeou, E.P. Favvas, F.K. Katsaros, and K. Stamatakis, “Effect of copper and copper alginate treatment on wool fabric. Study of textile and antibacterial properties,” *Sur. Coatings Tech.*,” **235**, 24–31 (2013); doi.org/10.1016/j.surfcoat.2013.07.009.
26. Galani Irene, Priniotakis Georgios, Chronis Ioannis, Tzerachoglou Anastasios, Plachouras Diamantis, Chatzikonstantinou Marianthi, Westbroek Philippe, and Souli Maria, “Copper-coated textiles: armor against MDR nosocomial pathogens,” *Dia. Mic. Infectious Disease.,* **85**, 205–209 (2016); doi.org/10.1016/j.diagmicrobio.2016.02.015.
27. M. Messaoud, E. Chadeau, C. Brunon, T. Ballet, L. Rappenne, F. Roussel, D. Leonard, N. Oulahal, and M. Langlet, “Photocatalytic generation of silver nanoparticles and application to the antibacterial functionalization of textile fabrics,” *J. Photo. Photo. A: Chemistry*., **215**, 147–156 (2010); doi.org/10.1016/j.jphotochem.2010.08.003.
28. A. Allion-Maurer, C. Saulou-Bérion, R. Briandet, S. Zanna, N. Lebleu, P. Marcus, P. Raynaud, B. Despax, and M. Mercier-Bonin, “Plasma-deposited nanocomposite polymer-silver coating against,” *Escherichia coli* and *Staphylococcus aureus*: Antibacterial properties and ageing,” *Sur. Coatings Tech.*, **281**, 1–10 (2015); doi.org/10.1016/ j.surfcoat.2015.09.025.
29. M. Ferraris, S. Perero, S. Ferraris, M. Miola, E. Vernè, S. Skoglund, E. Blomberg, and I. Odnevall Wallinder, “Antibacterial silver nanocluster/silica composite coatings on stainless steel,” *Applied Sur. Sci.*. **396**, 1546–1555 (2017); doi.org/10.1016/j.apsusc.2016.11.207.
30. C.H. Xue, J. Chen, W. Yin, S.T. Jia, and J.Z. Ma, “Superhydrophobic conductive textiles with antibacterial property by coating fibers with silver nanoparticles,” *Applied Sur. Sci.*, **258**, 2468–2472 (2012); doi.org/10.1016/j.apsusc.2011.10.074.
31. K. Jyoti and A.E. Singh, “Evaluation of antibacterial activity from phytosynthesized silver nanoparticles against medical devices infected with *Staphylococcus spp*.,” *J. Taibah Uni. Med. Sci.*, **12**, 47–54 (2017); doi.org/10.1016/j.jtumed.2016.08.006.
32. S.M. Dizaj, F. Lotfipour, M. Barzegar-Jalali, M.H. Zarrintan, and K. Adibkia, “Antimicrobial activity of the metals and metal oxide nanoparticles,” *Mater. Sci. Eng. C.*, **44**, 278–284 (2014); doi.org/10.1016/j.msec.2014.08.031.
33. P. Dhandapani, A.S. Siddarth, S. Kamalasekaran, S. Maruthamuthu, and G. Rajagopal, “Bio-approach: Ureolytic bacteria mediated synthesis of ZnO nanocrystals on cotton fabric and evaluation of their antibacterial properties,” *Carbohydr. Polym.*, **103**, 448–455 (2014); doi:10.1016/j.carbpol.2013.12.074.
34. A. Sirelkhatim, S. Mahmud, A. Seeni, N.H.M. Kaus, L.C. Ann, S.K.M. Bakhori, H. Hasan, and D. Mohamad, “Review on Zinc Oxide Nanoparticles: Antibacterial Activity and Toxicity Mechanism,” *Nano-Micro Lett.*, **7**, 219–242 (2015); doi.0.1007/s40820-015-0040-x.